Fire emissions in tropical forests: refining the SPITFIRE model using remote sensing data

Imogen Nancy Fletcher[1]
Guillermo Murray-Totarolo[1]
Pierre Friedlingstein[1]
Andre Lima[2]
Yosio Edemir Shimabukuro[2]
Luiz Eduardo Oliveira e Cruz de Aragão[3]

[1]University of Exeter – College of Engineering, Mathematics and Physical Sciences
Harrison Building, University of Exeter, North Park Road, Exeter, UK, EX4 4QF
{inf201, gnm202, p.friedlingstein}@exeter.ac.uk

[2] Instituto Nacional de Pesquisas Espaciais - INPE
Caixa Postal 515 - 12245-970 - São José dos Campos - SP, Brasil
{yosio, andre}@ltid.inpe.br

[3]University of Exeter – College of Life and Environmental Sciences
Amory Building, University of Exeter, Rennes Drive, Exeter, UK, EX4 4RJ
l.aragao@exeter.ac.uk

Abstract. Tropical fires are the most poorly represented fire type in Dynamic Global Vegetation Models (DGVMs), due to an incomplete understanding of the factors driving them. As the time period increases for which remote sensing fire data is available, it becomes possible to assess long-term trends and distinguish between natural interannual variability and the effects of changes in anthropogenic drivers of fire. The SPITFIRE model captures the broad features of global fire regimes, but includes several processes that rely heavily on the accuracy of the input data, products of earlier calculations, and prescribed parameters. In this paper, we develop two alternative approaches for calculating fire danger and burnt areas, whose substitution into SPITFIRE would increase computational efficiency and reduce the required number of weakly constrained input variables and datasets. We first model fire danger as a function of water stress and fuel availability proxies. Second, we test a new burnt area model using a Pareto distribution, which relies on fire counts, thus eliminating the need for rate of fire spread information. Parameters for the fire danger model have yet to be estimated, but the structure is plausible. The burnt area model performs well for Amazonia for a range of grid resolutions and parameter estimates; coarse resolutions produce the most accurate results. More data is required to calibrate the equations across the tropics. These changes could potentially improve predictions of which areas are at risk of burning, but not the extent of damage to standing biomass: this will require further model improvements.

Keywords: Burnt area, Pareto, Fuel limitation, Moisture, Remote Sensing.

1. Introduction

Fires play a major role in the global carbon cycle. At the end of the 20th century, about 600 Mha are burnt globally each year, with approximately 86% of these burns occurring in tropical savannas, and burning in tropical forests is increasing exponentially (Mouillot and Field, 2005). However, tropical fires are the most poorly represented fires in existing Dynamic Global Vegetation Models (e.g., Prentice et al., 2011), due to an incomplete understanding of the factors driving them.

As an increasing amount of remote sensing data on burned area and fire occurrence is becoming available, our capacity to accurately model fires is improving. We are only now beginning to have data from a sufficiently long time-period to be able to assess long-term trends, and to distinguish between natural interannual variability and the effects of changing drivers of the fire regime. Fire products from the Moderate Resolution Imaging Spectroradiometer (MODIS), for instance, are available from 2000 onwards (Justice et al., 2002).

The SPITFIRE model, designed by Thonicke et al. (2010), is a modification of the Reg-FIRM model (Venevsky et al., 2002) and its predecessor, Glob-FIRM (Thonicke et al., 2001). Although currently one of the most widely used fire models in DGVMs, SPITFIRE still has some crucial limitations, and we believe that there are several processes that rely too heavily on the accuracy of the input data, products of earlier calculations, and prescribed parameters. Our work, therefore, suggests alternative frameworks for two of these processes, namely the calculation of fire danger, and hence the number of fires that occur for a given region and time period, and the estimation of the resulting burnt area.

There are currently three commonly-used weather-based indices of fire danger (FDI): the Nesterov Index (NI), the McArthur Forest Fire Danger Index (FFDI, Noble et al. (1980)) and the Canadian Forest Fire Weather Index (FFWI). SPITFIRE currently uses the NI, which requires the input of daily maximum and minimum temperatures (^{o}C). The NI is then used in conjunction with information about the quantities of different fuel classes and prescribed surface-area-to-volume ratios and moistures of extinction to calculate the fire danger index.

In the tropics, the amplitude of temperature variation is small and the best predictor for fire occurrence may be a combination of water stress and fuel loads. It has been shown that fire activity peaks at a certain level of precipitation, and is small for both large and small amounts of annual precipitation (van der Werf et al., 2008, Prentice et al., 2011). The suggested explanation for this is that fire is limited by both water and fuel availability, so for sparsely vegetated regions, a dry year results in low net primary productivity (NPP) and therefore there is little that can burn.

In contrast to the FDI model, the current method for calculating burnt area, A_b, in SPITFIRE appears at first glance to be relatively straightforward, as shown by Equation (1), where $E(n_f)$, $\bar{a}_f$, A are the expected number of fires per unit area and time, mean fire area and grid cell area, respectively.

$$A_b = E(n_f) \cdot \bar{a}_f \cdot A \quad (1)$$

The value of $E(n_f)$ is the minimum of the FDI and the number of potential ignitions from both lightning and anthropogenic sources. The mean fire area is a complex process that cannot be estimated without the following data: wind speed; reaction intensity of the fire; the propagation flux ratio; fuel bulk density; the effective heating number; heat of pre-ignition; and, the FDI. Full details of these variables can be found in Thonicke et al. (2010). With so many input parameters and variables, the propagated calculation error tends to be high.

An alternative solution for the burned area problem is to replace the complex mechanistic model with a simple statistical description of the distribution of burned area within a grid cell, based on a probability density function. It has been shown for many regions that fire size-distributions follow either a power-law (e.g., Malamud et al., 1998), Pueyo et al., 2010, Moreno et al., 2011) or Pareto (e.g., Schoenberg et al., 2003) behaviour, meaning that the probability that a fire is of size A (power) or greater than size A (Pareto) is proportional to A^{-b}, for some value of b.

The present work will focus on developing alternative frameworks for two of these processes, namely the calculation of fire danger, and therefore the number of fires that occur for a given region and time period, and the estimation of the resulting burnt area. Specifically, we will present an analysis of the calculation of the FDI using only precipitation, evapotranspiration and NPP. This will translate to the maximum number of fires that could occur. Moreover, we will demonstrate an alternative estimate of burnt area that requires only fire count data and biome-specific parameters. With these modifications we aim to improve computational efficiency of carbon emission modelling without heavily compromising on accuracy, and to reduce the risk of errors being amplified through multiple calculations.

2. Methodology

Much of the methodology depends on the characteristics of the data available. For instance, the spatial resolution, the time period considered, and the datasets used depends on which DGVM the SPITFIRE model is coupled to. In sections 2.1 and 2.2, the methods used to calculate the required products are explained in general terms, and datasets with which to assess the model validity and calibrate the parameters are presented.

2.1 Fire danger

Since the majority of tropical fires occur during the local dry season, with the exception perhaps of a few that are ignited anthropogenically, we first need to identify the length and timing of each dry season. If we define the dry season as the period during which the amount of evapotranspiration exceeds the amount of precipitation, we can then calculate both the dry season length (DSL) and the cumulative water deficit of the dry season (CWD), as a measure of the intensity of the dry season. The CWD is defined as in Equation 2, for a given DSL d (days), daily precipitation $P(t)$, and daily evapotranspiration $E(t)$.

$$CWD = \sum_{t=0}^{t=d} P(t) - E(t) \quad (2)$$

If evapotranspiration data for tropical forests is not available, or thought to be unreliable, it can be replaced by a constant mean evapotranspiration value of 100mm, according to the approach taken by Aragão et al. (2007). The total NPP of the preceding dry season is used as a proxy for fuel availability.

If we define the fire danger of a grid cell as the expected maximum number of fires that can occur given certain moisture and fuel conditions, then we would expect to be able to express this as a function of CWD, DSL and wet season NPP. This FDI can then be taken together with the ignition potential (as already defined in SPITFIRE) to produce an estimate of the actual number of fires that occur in a grid cell in a given dry season. Daily fire counts would be obtainable through interpolation of the total fire counts, weighted by the daily increase in water stress.

To provide an initial indication of the plausibility of the proposed fire danger model, we used the MODIS Global Monthly Fire Location Product (MCD14ML) (Giglio, 2010), the CRU TS3.1 global precipitation data (Jones, 2008), and NPP and Evapotranspiration timeseries from the TRIFFID model, as calculated by the TRENDY project (Sitch et al., submitted). All data is scaled to a 1^{o}x1^{o} grid, interpolated to a daily time step, where necessary (the fire product data is available on a daily basis), and restricted to the region between 25^{o}N and 25^{o}S, since we are interested only in the tropics at this point. It is possible, however, that the results will be applicable on a global scale.

2.2 Burnt area

Using data that details the sizes of burnt areas (Lima et al., 2009), the value of parameter b can be estimated for any size grid cell which experiences more than 3 fires in the desired time period, by calculating the gradient of the linear model described in Equation (3), where $n_{X>A}$ is the observed number of burn scars whose size X is larger than A, and a is constant.

$$\log n_{X>A} = a - b \log A \quad (3)$$

For ease of calculation, we define size as the number of 500m x 500m pixels rather than area in km^2, and convert to metric units at the end, but this does not affect the results. If a burn scar lies across the boundaries of two or more grid cells, it is attributed to the grid cell in which the largest proportion of the burn scar can be found.

To estimate burnt area, we need to know only the values of parameters *a* and *b*, and the total number of fires. If the parameter *a* is not available - for instance, if we choose to use values of *b* as estimated in the literature for various different regions – then *a* can be approximated to log(*n*), where *n* is the total number of fires. The maximum possible fire size, *s*, is dependent on the x-intercept of Equation 3, following the relationship

$$s = \exp(\frac{a}{b}) \tag{4}$$

and rounded to the nearest integer. The expected number of fires larger than each size $A \in (1,s)$, denoted $E(n_{X>A})$, is

$$E(n_{X>A}) = \exp(a - b \cdot \log(A)) \tag{5}$$

By taking the difference between the values of $E(n_{X>A})$ for each consecutive value *A*, we can calculate the expected number of fires that are of size *A*, and hence produce an estimate of the total area burnt.

Assessing the validity of the proposed burnt area model is difficult, due to the limited amount of available fire size data. To perform this analysis, we use the burned area map produced for the year 2005 by Lima et al. (2009), which covers Brazilian Amazonia at a 500 m x 500 m spatial resolution. In order to implement this model on a global scale, or even across the tropics, a more extensive dataset must be used. Because the Pareto parameters vary across different biomes, it should be possible to produce a formula to estimate their values based on local land cover or vegetation type. In the meantime, estimates from the literature can be used to apply the Pareto burnt area model to individual regions, such as Alberta, Canada (Cumming, 2001) and Los Angeles County (Schoenberg et al., 2003).

In order to incorporate such a model into a fire model like SPITFIRE, burnt area will need to be estimated within grid cells. Larger grid-cells or longer time intervals will provide more data points for parameter estimation, and therefore will result in more accurate values and an increase in the significance of the linear models. We repeat the analysis for three different grid resolutions (2^ox2^o, 1^ox1^o and 0.5^ox0.5^o) to assess the effect of the choice of resolution on the accuracy of the method. We present a more in-depth analysis of the model fit for a 1^ox1^o resolution, since most DGVMs calculate variables at this, or a finer, resolution.

3. Results and Discussion

Initial analyses confirm that CWD and total wet season NPP are suitable proxies for water and fuel availability, respectively. For dry seasons shorter than approximately 6 months, where the CWD is below about 160mm, fire events are limited by an excess of fuel moisture. For longer dry seasons, the water stress is sufficiently large and no longer restricts burning, but NPP levels lower than 500 gC/m^2 as a result of the shorter wet season mean that there is a limited amount of fuel that can burn. While the mean NPP is also below 400 gC/m^2 for grid cells that experience a dry season of less than 3 months, the fire regime is more limited by moisture than by fuel availability in these regions. These interactions can be seen clearly in Figure 1.

The exact relationships between these variables are, as yet, unclear. However, statistical models are being developed by this group, so that we can quantify the effects of water and fuel availability on fire. Only the highest *x* % of fire counts for each NPP and CWD partition, for some arbitrary value of *x*, should be used to fit the model, since we are not including ignition data. Once a suitable model has been found, the suitability of different values of *x* can be investigated. Parameter estimates from the resulting model can be used in the new SPITFIRE fire danger model.

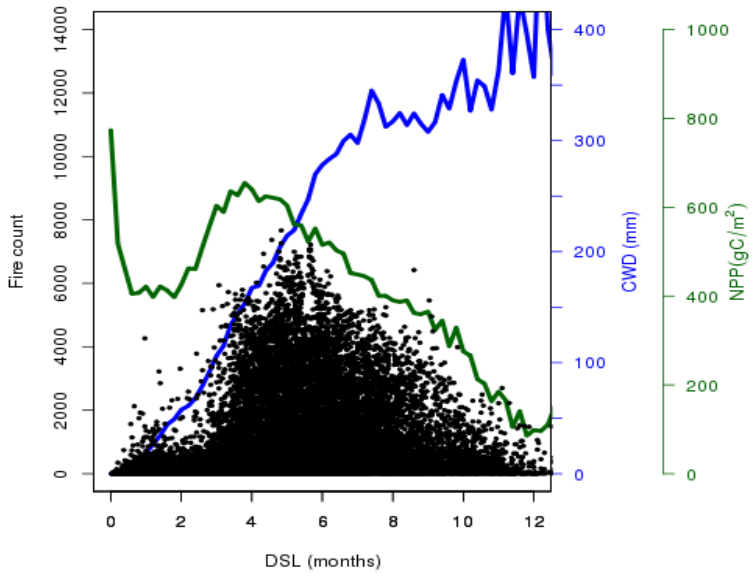

Figure 1. Fire counts (black dots) against dry season length for every dry season for every grid cell in the tropical region (25°N and 25°S). The green and blue lines are the corresponding mean NPP and CWD for every 0.2-month division of DSL, respectively.

For the Amazonian fire size and frequency data, size is an integer-valued variable, representing the number of adjacent pixels that make up each fire event. Pixels are considered adjacent if both the latitudinal and the longitudinal distances between them are equal to 500m. Based on a total of 12,030 distinct burn scars, ranging from 1 to 135.25 km^2 in size, fire behaviour in the Amazon can be described by the Pareto distribution (Figure 2). Initial analyses showed that the power-law distribution described much of the fire size behaviour for this data, but not as well as the Pareto distribution. The linear model of $n_{X>A} \sim A$ is highly significant ($R^2 = 0.98$, p-value $< 2.2 \times 10^{-16}$). The model, however, overestimates the number

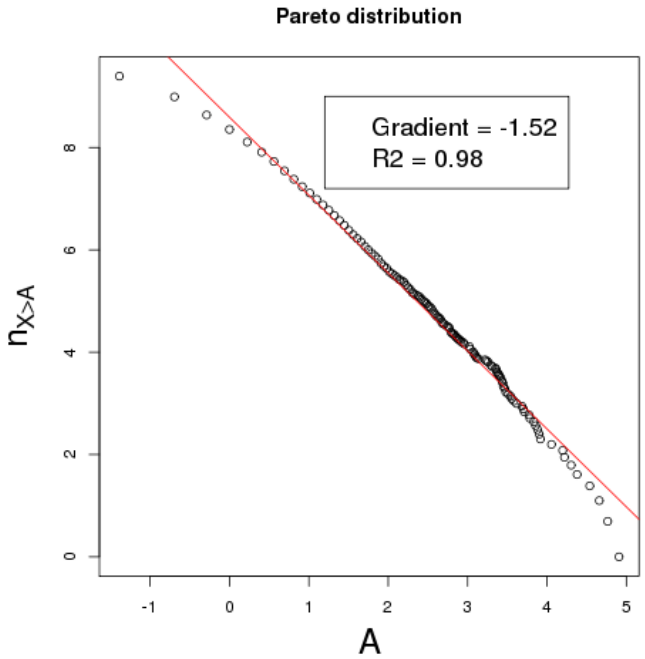

Figure 2. Log-scale plot of the number of fires greater than or equal to size A, against, A, where A is the number of 500m x 500m size pixels. The corresponding linear model fit is shown in red.

of very large fires and underestimates small fires, with a root mean square error (RMSE) of 0.215 on the log-scale (equivalent to 1.24 fire events). This could be attributed to data collection error, as small burnt areas are difficult to detect, and large fire events can be mistaken for several smaller fires.

Investigation of the model accuracy when fitting it to grid cells of varying sizes shows that coarser grids result in higher coefficients of determination (R^2) and a larger proportion of fire-affected grid cells having significant model fits (Table 1). Coarser resolutions therefore reduce the amount of data that is lost due to grid cells having too few data points to fit a Pareto model, and improve the model fit. Additionally, the same applies to choosing time intervals over which to calculate parameters: the current data is static, rather than a time series, but in general, the longer the time-step, the more likely it is that there will be enough observations in each grid cell to produce adequate parameter estimates.

Table 1. Model statistics for different grid resolutions.

Grid resolution	**Mean parameter estimates**		**Mean R^2**	**Number of grid-cells with burn scars**	**Percentage of grid-cells with burn scars that have significant parameter estimates**
	a	***b***			
0.5^o x 0.5^o	2.53 ± 1.55	0.93 ± 0.46	0.86	529	76%
1^o x 1^o	3.46 ± 1.90	1.11 ± 0.48	0.87	205	86%
2^o x 2^o	4.58 ± 2.27	1.27 ± 0.49	0.88	75	93%

For a standard 1^ox1^o resolution, we tested the model fit using both the value of *a* as estimated in the linear model, and the approximation for *a*, log(*n*), as described in the methods. While both parameterizations appear to provide good estimates for grid cells in which less than roughly 125 km^2 (approximately one hundredth of a grid cell) burns, it is apparent from Figure 3 that using the model intercept results in an overestimation, and log(*n*) in an underestimation, for areas with larger burn areas. Taking the means of the values predicted using each of these parameterizations, results in a good set of predictions, with the exception of only a few outliers. The fitted intercept value may not always be available, for instance, when using estimates of parameter *b* from the literature, in which case a scaling factor for the value of *a* may need to be found. However, it is important to realise that the observed values themselves may not be entirely accurate, due to the difficulties that arise when identifying burn scars.

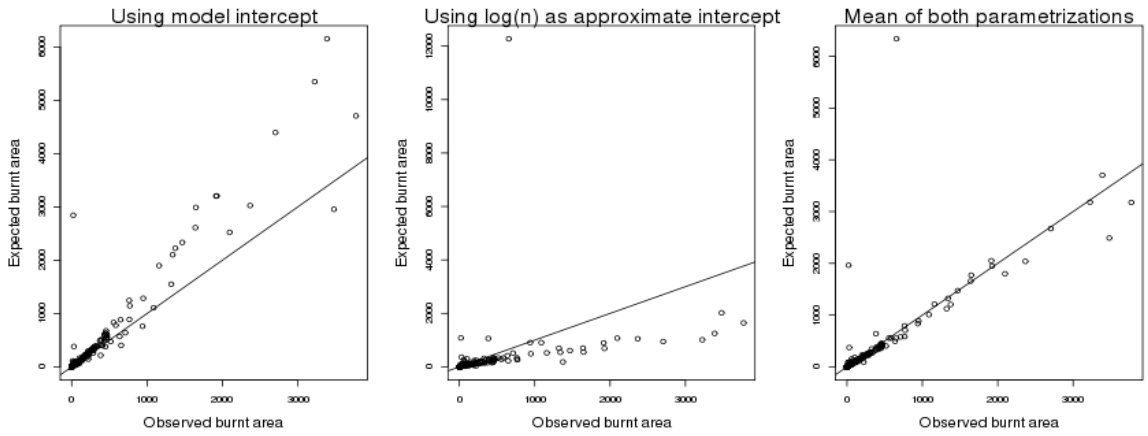

Figure 3. Predicted burnt area against observed burnt area (number of pixels), using the intercept estimated from the linear model (left), log(*n*) (middle), and the mean of these two values (right) as the value of *a*.

4. Conclusions

Both of the proposed sets of calculations have been shown to be based on robust assumptions of ecological processes, and both represent a considerable simplification of the SPITFIRE model, yet still give realistic results in terms of fire danger index and burned areas. As such, their implementation would result in a significant increase in computational efficiency.

Ongoing research is also being carried out to test the effect of the implementation of these new submodels, both individually and in conjunction with one another, on the performance of SPITFIRE. Current versions of SPITFIRE that are in use have been modified according to the DGVMs they are coupled with, so we are working to incorporate both the original SPITFIRE equations and the new models into the Joint UK Land Environment Simulator (JULES) model. This should enable us to compare the two versions of the FDI and burnt area processes against each other, and against the GFED3 burnt area data (Giglio et al., 2010). Similarly, the interannual variability of the model predictions can be investigated, to see how the models capture, for instance, increased fire counts in Amazonia during El Niño events. The efficacy of the suggested burnt area model structure will be investigated across the tropics and globally, using burned area products derived from MODIS (Roy et al., 2008). We have shown here that the statistical representation of burned area performs well for Amazonian forests when the value of parameter *b* is calculated directly from the data. The effect of estimating b using land cover data on the final burnt area estimates is still uncertain.

The modular structure of SPITFIRE would make the incorporation of both of these processes a relatively straightforward task. However, despite being able to eliminate the complex rate of spread calculation from the burnt area estimates, the former is still needed for other model processes, including the extent of crown and cambial damage, the surface fire intensity, and the amount of biomass burnt. These two new submodels therefore have the potential to facilitate predictions of which areas will be affected by fire, but there is scope for further modifications to the SPITFIRE model to improve forecasts of the extent of fire damage to an ecosystem.

Acknowledgements

The authors would like to thank Stephen Sitch (University of Exeter) and Chris Huntingford (Centre for Ecology & Hydrology) for the TRIFFID-TRENDY data, and the UK Natural Environment Research Council (NERC) (NE/F015356/2 and NE/l018123/1) and the University of Exeter, Climate Change and Sustainable Futures group for the first author's PhD studentship.

References

Aragão, L. E. O. C.; Malhi, Y.; Roman-Cuesta, R. M.; Saatchi, S.; Anderson, L. O.; Shimabukuro, Y. E. Spatial patterns and fire response of recent Amazonian droughts. **Geophysical Research Letters**, v. 34, 2007.

Cumming, S. G. A parametric model of the fire-size distribution. **Canadian Journal of Forest Research,** v. 31, p. 1297-1303, 2001.

Giglio, L. **MODIS Collection 5 Active Fire Product User's Guide Version 2.4.** Science Systems and Applications, Inc., University of Maryland, Department of Geography, 2010.

Giglio, L.; Randerson, J. T.; van der Werf, G. R.; Kasibhatla, P. S.; Collatz, G. J.; Morton, D. C.; DeFries, R. S. Assessing variability and long-term trends in burned area by merging multiple satellite fire products. **Biogeosciences**, v. 7, p. 1171-1186, 2010.

Justice, C. O.; Giglio, L.; Korontzi, S.; Owens, J.; Morisette, J. T.; Roy, D.; Descloitres, J.; Alleaume, S.; Petitcolin, F.; Kaufman, Y. The MODIS fire products. **Remote Sensing of Environment**, v. 83, p. 244-262, 2002.

Lima, A.; Shimabukuro, Y. E.; Adami, M.; Freitas, R. M.; Aragão, L. E.; Formaggio, A. R.; Lombardi, R. Mapeamento de cicatrizes de queimadas na amazônia brasileira a partir da aplicação do modelo linear de mistura espectral em imagens do sensor MODIS. **Anais do XIV Simpósio Brasileiro de Sensoriamento Remoto, Natal,** p. 5925 - 5932, 2009.

Malamud, B. D.; Morein, G.; Turcotte, D. L. Forest Fires: An Example of Self-Organized Critical Behavior. **Science**, v. 281, p. 1840-1842, 1998.

Moreno, M. V.; Malamud, B. D.; Chuvieco, E. Wildfire Frequency-Area Statistics in Spain. **Procedia Environmental Sciences**, v. 7, p. 182-187, 2011.

Mouillot, F.; Field, C. B. Fire history and the global carbon budget: a 1x1 fire history reconstruction for the 20th century. **Global Change Biology**, v. 11, p. 398-420, 2005.

Noble, I. R.; Gill, A. M.; Bary, G. A. V. McArthur's fire-danger meters expressed as equations. **Australian Journal of Ecology**, v. 5, n. 2, p 201-203, 1980.

Prentice, I. C.; Kelley, D. I.; Foster, P. N.; Friedlingstein, P.; Harrison, S. P.; Bartlein, P. J. Modeling fire and the terrestrial carbon balance. **Global Biogeochemical Cycles**, v. 25, 2011.

Pueyo, S.; de Alencastro Graça, P. M. L.; Barbosa, R. I.; Cots, R.; Cardona, E.; Fearnside, P. M. Testing for criticality in ecosystem dynamics: the case of Amazonian rainforest and savanna fire. **Ecology Letters**, v. 13, p. 793-802, 2010.

Roy, D. P.; Boschetti, L.; Justice, C. O.; Ju, J. The collection 5 MODIS burned area product - Global evaluation by comparison with the MODIS active fire product. **Remote Sensing of Environment,** v. 112(9), p. 3690-3707, 2008.

Schoenberg, F. P.; Peng, R.; Woods, J. On the distribution of wildfire sizes. **Environmetrics**, v. 14, p. 583-592, 2003.

Sitch et al., Uncoupled DGVMs from the TRNDY/RECCAPP project, using S2 (CO2 + Climate) runs. **Personal communication.** (Submitted)

Sitch, S.; Friedlingstein, P.; Gruber, N.; Steve, J. S.; Murray-Tortarolo, G.; Ahlström, A.; Doney, S. C.; Graven, H.; Heinze, C.; Huntingford, C.; Levis, S.; Levy, P. E.; Lomas, M.; Poulter, B.; Viovy, N.; Zaehle, S.; Zeng, N.; Arneth, A.; Bonan, G.; Bopp, L.; Canadell, J. G.; Chevallier, F.; Ciais, P.; Ellis, R.; Gloor, M.; Peylin, P.; Piao, P.; Le Quéré, C.; Smith, B.; Zhu, Z.; Myneni, R. Trends and drivers of regional sources and sinks of carbon dioxide over the past two decades. **Biogeosciences**, submitted, 2012.

Thonicke, K.; Spessa, A.; Prentice, I. C.; Harrison, S. P.; Dong, L.; Carmona-Moreno, C. The influence of vegetation, fire spread and fire behaviour on biomass burning and trace gas emissions: results from a process-based model. **Biogeosciences**, v. 7, p 1991-2011, 2007.

Jones, P.; Harris, I. University of East Anglia Climatic Research Unit (CRU) CRU Time Series (TS) high resolution gridded datasets, [Internet]. NCAS British Atmospheric Data Centre, 2008. Available from http://badc.nerc.ac.uk/view/badc.nerc.ac.uk__ATOM__dataent_1256223773328276, accessed 12 Nov 12.

van der Werf, G. R.; Randerson, J. T.; Giglio, L.; Gobron, N.; Dolman, A. J. Climate controls on the variability of fires in the tropics and subtropics. **Global Biogeochemical Cycles**, 22, 2008.